Applied Catalysis B: Environmental 130–131 (2013) 152–162

Contents lists available at SciVerse ScienceDirect

Applied Catalysis B: Environmental

journal homepage: www.elsevier.com/locate/apcatb

Selective catalytic oxidation of ammonia to nitrogen over Mg-Al, Cu-Mg-Al and Fe-Mg-Al mixed metal oxides doped with noble metals

Lucjan Chmielarz[a,*], Magdalena Jabłońska[a], Adam Strumiński[a], Zofia Piwowarska[a], Agnieszka Węgrzyn[a], Stefan Witkowski[a], Marek Michalik[b]

[a] Jagiellonian University, Faculty of Chemistry, Ingardena 3, 30-060 Kraków, Poland
[b] Jagiellonian University, Institute of Geological Sciences, Oleandry 2a, 30-063 Kraków, Poland

ARTICLE INFO

Article history:
Received 22 July 2012
Received in revised form 30 October 2012
Accepted 5 November 2012
Available online 12 November 2012

Keywords:
Selective catalytic oxidation (SCO) of ammonia
Hydrotalcite-like materials
Mixed metal oxides
Noble metals

ABSTRACT

Mg-Al, Cu-Mg-Al and Fe-Mg-Al mixed oxides, were obtained by thermal decomposition of synthetic hydrotalcite-like materials and, in the next step, were modified with selected noble metals (Pt, Pd, Rh) by incipient wetness impregnation method. The process of thermal decomposition of hydrotalcite-like materials into metal oxide systems was studied by thermogravimetry method combined with the on-line analysis of gaseous products of the sample decomposition (TG–DTA-QMS). The obtained catalysts were studied with respect to chemical composition (EDS), structure (XRD, UV–vis–DRS), morphology (STEM), surface area (BET) and redox properties (H_2-TPR). Metal oxide catalysts obtained from the hydrotalcite-like precursors were characterized by high dispersion of transition metals (Cu, Fe), which were present mainly in the form of monomeric or small aggregated species dispersed in the Mg-Al oxide matrix. Noble metals, as it was shown by STEM studies, were rather uniformly dispersed on the surface of the samples. The obtained samples were tested as catalysts of the selective catalytic oxidation (SCO) of ammonia to nitrogen. The Cu-Mg-Al oxide catalyst was active in the low-temperature SCO process, while the Fe-containing sample was found to operate in the high temperature range. Modification of these catalysts with noble metals significantly decreased temperature of the ammonia oxidation but also decreased the selectivity to nitrogen. The best catalytic properties were obtained for the Cu-Mg-Al oxide catalyst modified with small amount of platinum (0.2 wt%), which operated at relatively low temperature with high selectivity to nitrogen.

1. Introduction

The increasing problem of atmospheric pollution by various N-containing compounds, such as NO, N_2O, NO_2 and NH_3, has resulted in stricter regulations on their emission. Many chemical processes use ammonia as a reactant or produce ammonia as a by-product (e.g. nitric acid and nitrogen fertilizer production, urea manufacturing, hydrodenitrification process, DeNOx process). The selective catalytic oxidation (SCO) of ammonia by oxygen to nitrogen and water vapour, according to the reaction given below (1), is one of the most promising methods for the removal of NH_3 from oxygen containing waste gases.

$$4NH_3 + 3O_2 = 2N_2 + 6H_2O \quad (1)$$

N_2O and NO are the main by-products of this process. The effective SCO catalysts should operate in a relatively low temperature range and additionally should selectively direct the reaction to the formation of nitrogen and water vapour.

Various transition metal oxides, including CuO, Fe_2O_3, Co_3O_4, MnO_2 MoO_3, V_2O_5 [e.g. 1–6], were tested as catalysts for the SCO process. Among them the catalysts containing copper and iron were found to be one of the most interesting systems.

Our previous studies have shown that hydrotalcite-like materials are very promising precursors of the catalysts for various reactions: DeNOx [7,8], DeN$_2$O [9], VOCs incineration [10] and SCO of ammonia [11,12]. Hydrotalcites, also called layered double hydroxides (LDHs), are characterized by the brucite-like structure [$Mg(OH)_2$], where the octahedra of Mg^{2+} (six-coordinated to OH^-) form doubled layers. Part of Mg^{2+} ions is replaced by trivalent cations (e.g. Al^{3+}), what results in a positive charging of the brucite-like layers. This positive charge is compensated by anions (e.g. CO_3^{2-}, NO_3^-), which together with water molecules are located in the interlayer space of the material. Furthermore, some of the Mg^{2+} as well as Al^{3+} ions can be replaced by other di- (e.g. Cu^{2+}) and trivalent- (e.g. Fe^{3+}) cations, respectively. Calcination of the hydrotalcite precursors results in their decomposition and formation of thermally stable mixed metal oxides characterized by a

* Corresponding author. Tel.: +48 126632006; fax: +48 126340515.
E-mail address: chmielar@chemia.uj.edu.pl (L. Chmielarz).

0926-3373/$ – see front matter © 2012 Elsevier B.V. All rights reserved.
http://dx.doi.org/10.1016/j.apcatb.2012.11.004

relatively high surface area and homogeneous distribution of metal cations. Taking into account these properties and additionally, a large number of various metals, which can be incorporated into the brucite-like layers, the hydrotalcite-like materials are very promising for the possible applications in catalysis.

Our previous studies [11] of the SCO reaction mechanism over the hydrotalcite originated metal oxide catalysts have shown that this process proceeds according to the *Internal Selective Catalytic Reduction* mechanism (*i-SCR*), which consists of the following steps:

(i) part of ammonia is oxidized to NO:

$$4NH_3 + 5O_2 = 4NO + 6H_2O \quad (2)$$

(ii) ammonia, unreacted in stage 2, reduces NO to N_2 (3a) or N_2O (3b):

$$4NH_3 + 4NO + O_2 = 4N_2 + 6H_2O \quad (3a)$$

$$4NH_3 + 4NO + 3O_2 = 4N_2O + 6H_2O \quad (3b)$$

Taking into account both reaction steps it could be concluded that the effective catalysts of the SCO process should be active in ammonia oxidation to NO (2) as well as in selective reduction of NO with ammonia to nitrogen (3a). Distribution of the N-containing reaction products should be strongly dependent on the relative activities of the catalyst in reaction (2), (3a) and (3b).

The presented studies are focused on development of active and selective, bi-functional catalysts for the SCO process. Selected noble metals (Pt, Pd, Rh) play a role of the components active in the oxidation of ammonia into NO, while mixed metal oxides containing cooper and iron are the components active in the selective reduction of NO with ammonia.

2. Experimental

2.1. Catalysts preparation

Mg-Al, Cu-Mg-Al and Fe-Mg-Al hydrotalcite-like materials with the intended atomic ratios of 71/29, 5/66/29 and 5/66/29, respectively, were synthesized by co-precipitation method using aqueous solutions of the following metal nitrates: $Mg(NO_3)_2{\cdot}6H_2O$ (Sigma), $Al(NO_3)_3{\cdot}9H_2O$ (Fluka), $Cu(NO_3)_2{\cdot}3H_2O$ (Merck), $Fe(NO_3)_3{\cdot}9H_2O$ (POCh). A solution of NaOH (POCh) was used as a precipitating agent. The mixture of nitrates and NaOH were simultaneously added to a vessel containing aqueous solution of Na_2CO_3 (POCh) at 60 °C. The pH of the mixture was maintained constant at 10.0 ± 0.2 by dropwise addition of NaOH solution. The obtained slurry was stirred at 60 °C for further 30 min, filtered, washed with distillated water and dried in air. The obtained samples were calcined at 600 °C for 12 h.

Calcined hydrotalcite-like materials were modified with selected noble metals (Pd, Pt, Rh) by incipient wetness impregnation method using methanol (Lach-ner) solutions of acetylacetonate complexes of these metals – $Pd(C_5H_7O_2)_2$, $Pt(C_5H_7O_2)_2$, $Rh(C_5H_7O_2)_2$ (all supplied by Accross). After impregnation, the samples were dried in air, crushed and calcined at 500 °C for 3 h. The obtained catalysts were kept in a desiccator in order to avoid the reconstruction of the hydroxide structure. The intended content of noble metals in the samples was 0.2 wt%, while the diameter of the catalyst grains was in the range of 160–315 μm.

2.2. Samples characterization

Thermal decomposition of the hydrotalcite samples was studied by termogravimetric method combined with on-line analysis of gaseous products (TG–DTA-QMS). The measurements were carried out using a Mettler Toledo 851^e thermobalance operated under a flow of pure argon (80 cm^3/min) in the temperature range of 25–1000 °C with a linear heating rate of 10 °C/min. The gases evolved during the thermal decomposition of the samples were continuously monitored with a quadruple mass spectrometer ThermoStar (Balzers) connected directly to the thermobalance.

The specific surface area of calcined hydrotalcites was determined by the BET method. The measurements were performed using Quantasorb Junior sorptometer (Ankersmit). Prior to the nitrogen adsorption at −196 °C the samples were outgassed in nitrogen atmosphere at 250 °C for 2 h.

The X-ray diffraction (XRD) patterns of the as-synthesised and calcined samples were recorded with a D2 Phaser diffractometer (Brucker) using Cu Kα radiation (λ = 1.54060 Å, 30 kV, 10 mA).

The chemical composition of the samples was determined by electron microprobe analysis using a HITACHI S-4700 instrument equipped with microanalysis system NORAN Vantage operated an accelerating voltage of 10 kV.

The STEM images were obtained with use of Tecnai Osiris 200 kV TEM/STEM system equipped with HAADF detector and Super-EDX windowless detector. STEM micrographs (512 × 512 points) were coupled with EDX data for presentation of distribution of the chosen element. Esprit software was used to control measurements and preparing the resulting images.

The redox properties of the catalysts were studied by temperature-programmed reduction method (H_2-TPR). The experiments were carried out in a fixed-bed flow microreactor from room temperature (RT) to 1100 °C with a linear heating rate of 5 °C/min. The gas mixture containing of 5 vol.% of H_2 diluted in argon was supplied into microreactor with a flow rate of 6 cm^3/min. Water vapour, which was a gas product of the metal oxides reduction, was removed from the effluent gas by means of a cold trap. Therefore, the signal of TCD detector (Valco) was associated only with consumption of hydrogen.

The species and aggregation state of the transition metals present in the samples was studied by UV–vis–DRS method. The UV–vis–DRS spectra were recorded using an Evolution 600 (Thermo) spectrophotometer. The measurements were performed in the range of 200–900 nm with a resolution of 1 nm.

2.3. Catalytic tests

The calcined hydrotalcites and their modifications with noble metals were tested in the role of catalysts for the selective catalytic oxidation of ammonia (SCO). The experiments were performed under atmospheric pressure in a fixed-bed flow reactor (i.d., 7 mm; l., 240 mm). The reactant concentrations were continuously monitored using a quadrupole mass spectrometer (PREVAC) connected to the reactor via a heated line. Prior to the reaction each sample of the catalyst (100 mg) was outgassed in a flow of pure helium at 600 °C for 1 h. The composition of the gas mixture at the reactor inlet was $[NH_3]$ = 0.5 vol.%, $[O_2]$ = 2.5 vol.% and [He] = 97 vol.%. Total flow rate of the reaction mixture was 40 cm^3/min, while a space velocity was about 15,400 h^{-1}. The reaction was studied at temperatures ranging from 50 to 500 °C. The intensities of the mass lines corresponding to all reactants and possible products were measured at a given temperature at least for 30 min after the reaction had reached a steady-state. The signal of the helium line served as an internal standard to compensate possible fluctuations of the operating pressure. The sensitivity factors of analyzed lines were calibrated using commercial mixtures of gases. The differences between the reactor inlet and outlet molar flows of the reactants were used to determine conversion of the reactants.

Additionally, the catalysts were tested in the process of selective catalytic reduction of NO with ammonia (NO-SCR, DeNOx). The catalytic experiments were performed in a fixed-bed flow

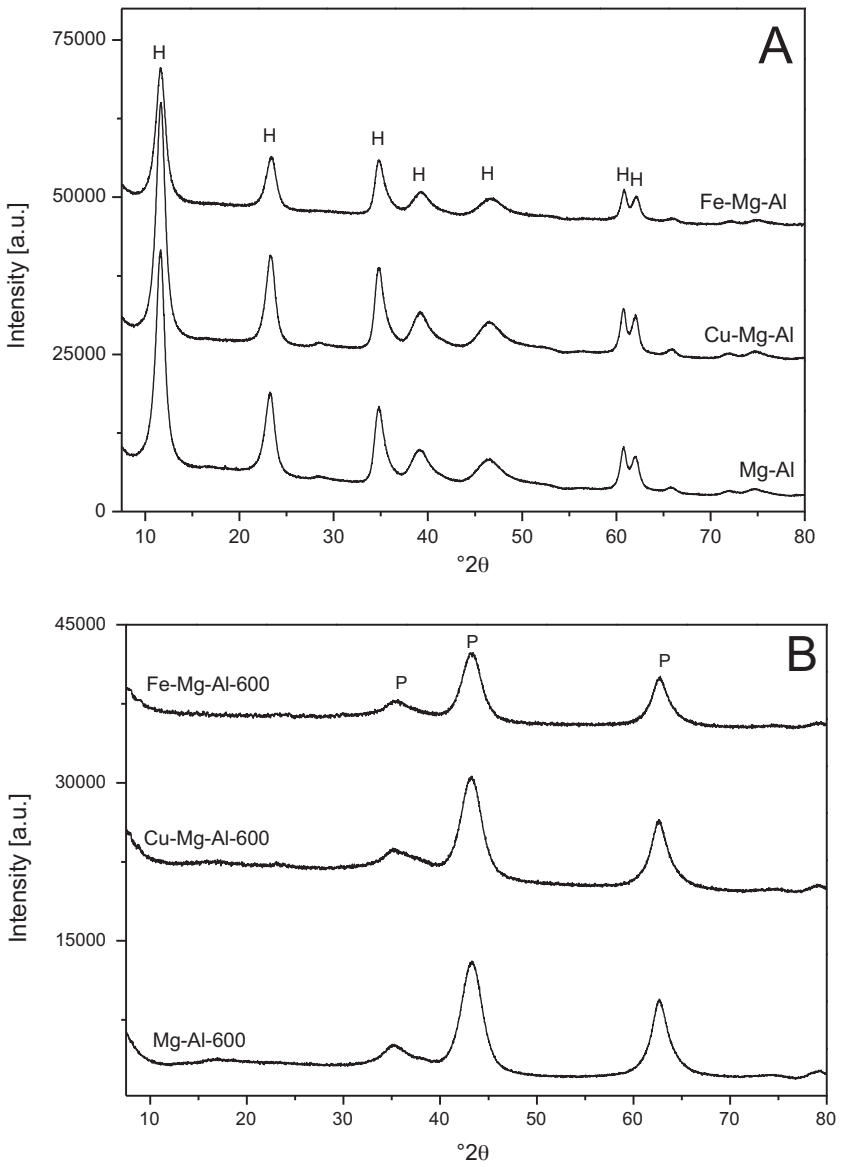

Fig. 1. X-ray diffraction patterns for hydrotalcite-like materials before calcination: Mg-Al, Cu-Mg-Al, Fe-Mg-Al (A) and after calcination: Mg-Al-600, Cu-Mg-Al-600, Fe-Mg-Al-600 (B); H – hydrotalcite, P – periclase, MgO.

microreactor (i.d., 7 mm; *l*, 240 mm). The reactant concentrations were continuously monitored using a quadrupole mass spectrometer (PREVAC) connected directly to the reactor outlet. Prior to the reaction tests, each sample (100 mg) of the catalyst was outgassed in a flow of pure helium at 600 °C for 1 h. The following composition of the gas mixture was used: [NO] = [NH_3] = 0.25 vol.%, [O_2] = vol. 2.5%. Helium was used as a balancing gas at a total flow rate of 40 cm^3/min, while a space velocity was about 15,400 h^{-1}.

3. Results and discussion

Powder XRD diffraction patterns obtained for the as-synthesized and calcined hydrotalcite-like materials are presented in Fig. 1. The as-synthesized samples exhibit the typical hydrotalcite-like structure belonging to the space group R3m in the trigonal symmetry [13]. Cell parameters and crystallite sizes of the hydrotalcite samples, determined from XRD measurements, are presented in Table 1. The cell parameter *c* for all the samples is about 2.3 nm, what is typical for hydrotalcites containing carbonates as the interlayer anions [11].

XRD patterns of the calcined samples contain only reflections typical of poorly crystallized MgO-type oxides (reflections at 36°, 43° and 63°). Any phases corresponding to noble metals (Pt, Pd, Rh) or their oxides (PtO, PdO, Rh_2O_3) were detected in diffractograms of the corresponding samples (results not shown).

STEM images of the Cu-Mg-Al-600-Pd, Cu-Mg-Al-600-Rh and Cu-Mg-Al-600-Pt samples are presented in Fig. 2. For all the samples deposited noble metals are present in the form of uniformly dispersed species.

The results of the thermogravimetric analysis of the hydrotalcite-like samples and the evolution of gaseous products released during their thermal decomposition, measured by QMS detector (*m*/*z*: 18 – H_2O, 44 – CO_2, 30 – NO), are shown in Fig. 3. Thermal decomposition of Mg-Al hydrotalcite proceeded in two main stages with a total mass loss of 45 wt%. The process of removal of interlayer water took place up to 250 °C. The second stage Mg-Al hydrotalcite decomposition, represented by two unresolved DTG minima at 344 and 381 °C, is related to the evolution of water vapour produced by dehydroxylation of —OH groups of the brucite-like layers and small amounts of CO_2 and

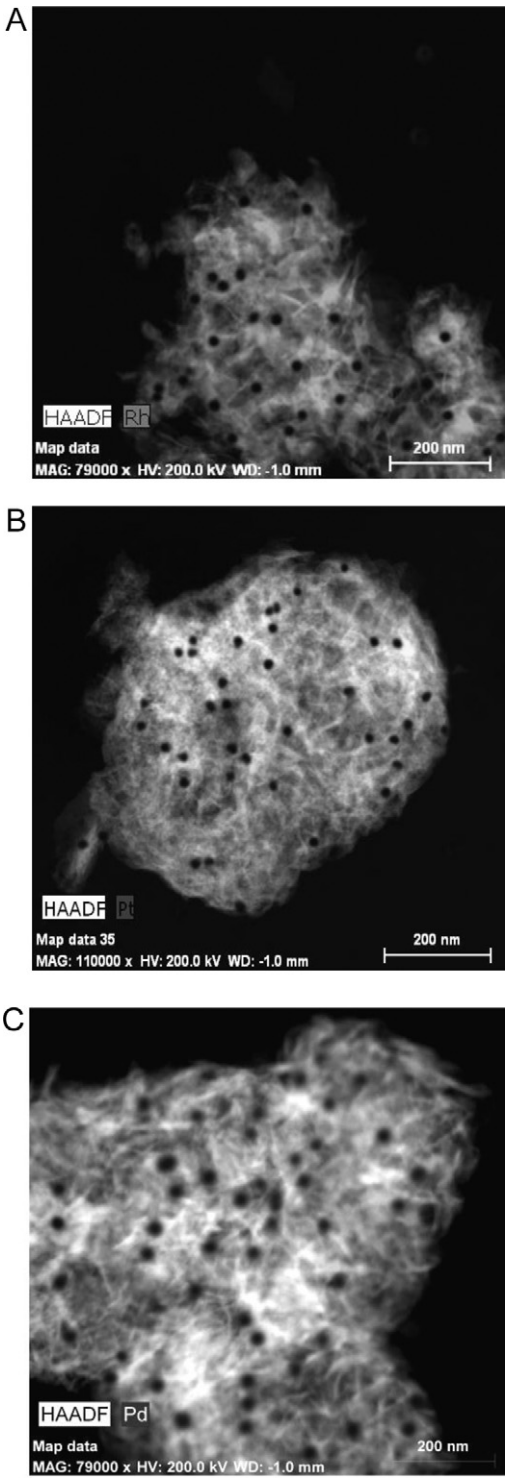

Fig. 2. STEM images of the Cu-Mg-Al-600-Rh (A), Cu-Mg-Al-600-Pt (B) and Cu-Mg-Al-600-Pd (C) samples. Black spots represent noble metal species distribution obtained by EDX. For clarity dimension of black spots is magnified.

NO, which are formed by thermal decomposition of the interlayer anions (CO_3^{2-} and NO_3^-). Therefore, it could be concluded that the positive charge of brucite-like layers in Mg-Al hydrotalcite is compensated mainly by carbonates, which decompose at lower temperatures than nitrates (Fig. 3A). Thermal decomposition of Cu-Mg-Al and Fe-Mg-Al hydrotalcites proceeded in a very similar way to the Mg-Al sample at temperature below 450 °C. Evolution of NO from the Mg-Al sample was detected at higher temperature (peak at 541 °C) than for the samples containing transition metals (peaks at 493 and 513 °C for Fe-Mg-Al and Cu-Mg-Al, respectively). Therefore, it seems that transition metals incorporated into the brucite-like layers decreased the stability of nitrate anions in the samples. Another difference is related to the high-temperature peak of CO_2 evolution, which is present at 637 °C for Cu-Mg-Al and at significantly lower temperature (about 590 °C) for the Mg-Al and Fe-Mg-Al samples. Therefore, it seems that copper is responsible for the stabilization of carbonates in the sample.

The specific surface area and chemical composition of the calcined Mg-Al, Cu-Mg-Al, Fe-Mg-Al samples are presented in Table 2. The assumed composition of the catalysts is very similar to that determined by chemical analysis. The main difference is related to the Mg/Al ratios, which are slightly lower than the assumed values.

It should be noted that calcined hydrotalcites containing copper or iron are characterized by lower surface area comparing to the calcined Mg-Al sample (Table 2). Deposition of noble metals decreased the specific surface area of the Mg-Al-600 sample. This effect was significantly less distinct for a series of the catalysts based on the Fe-Mg-Al-600 and Cu-Mg-Al-600 supports.

Only very weak and broad bands were found in the UV–vis–DR spectra recorded for the Mg-Al-600 sample and its derivatives containing rhodium and platinum (not shown). Therefore, the assignment of these bands is very difficult or even impossible and discussion based on these results would be very speculative. In this series of the samples only in a spectrum recorded for Mg-Al-600-Pd the intensive band at 250 nm with a shoulder at about 415 nm were found (Fig. 4). These bands are related to the charge-transfer (CTB) of Pd^{2+} ions and d–d transitions, respectively [14].

The UV–vis–DR spectrum recorded for the Cu-Mg-Al-600 sample consists of the maximum centred at 265 nm with a shoulder at about 350 nm and broad band above 600 nm (Fig. 4). The first peak is attributed to charge-transfer between mononuclear Cu^{2+} ion and oxygen, while the shoulder at about 360 nm can be ascribed to charge-transfer between Cu^{2+} and oxygen in oligonuclear $[Cu—O—Cu]_n$ species [15]. The band above 600 nm might arise due to Cu^{2+} d–d transition in an octahedral environment of bulky CuO crystallites [16]. The spectrum recorded for the Fe-Mg-Al-600 sample contains bands at 220, 280 and 350 nm together with a weak shoulder at around 450 nm (Fig. 4). The peaks observed below 300 nm are related to monomeric iron ions. The bands at 220 and 280 nm are related to monomeric Fe^{3+} species in tetrahedral and octahedral coordination, respectively [17]. The band located at 350 nm could be assigned to isolated Fe^{3+} ions incorporated into the periclase Mg(Fe,Al)O or Fe^{3+} ions in oligonuclear $(FeO)_n$ species [18]. The shoulder at about 450 nm can be assigned to the aggregated iron oxide clusters [19]. Therefore, it could be concluded that copper and iron is present mainly in the form of monomeric or small aggregated species dispersed in the Mg-Al oxide matrix.

Table 1
Structural parameters of hydrotalcite-like materials (before calcination).

Sample codes	Cell parameter a [nm]	Crystallite size Da [nm]	Cell parameter *c* [nm]	Crystallite size Dc [nm]
Mg-Al	0.3046	24	2.2888	15
Cu-Mg-Al	0.3050	26	2.2868	15
Fe-Mg-Al	0.3044	26	2.2829	14

Table 2
BET surface area and chemical composition of the calcined hydrotalcites.

Sample codes	S_{BET} [m^2/g]	Metal content [mol%]			
		Mg	Al	Transition metal	Noble metal
Mg-Al-600	173	69.80	30.20	0.00	0.0
Mg-Al-600-Pd	139	69.67	30.24	0.00	0.09 (Pd)
Mg-Al-600-Rh	148	69.79	30.12	0.00	0.09 (Rh)
Mg-Al-600-Pt	137	69.67	30.28	0.00	0.05 (Pt)
Cu-Mg-Al-600	132	64.91	30.55	4.54 (Cu)	0.0
Cu-Mg-Al-600-Pd	131	64.66	30.59	4.65 (Cu)	0.10 (Pd)
Cu-Mg-Al-600-Rh	130	64.86	30.52	4.52 (Cu)	0.10 (Rh)
Cu-Mg-Al-600-Pt	130	64.74	30.67	4.54 (Cu)	0.05 (Pt)
Fe-Mg-Al-600	130	64.66	30.76	4.58 (Fe)	
Fe-Mg-Al-600-Pd	125	64.54	30.78	4.60 (Fe)	0.08 (Pd)
Fe-Mg-Al-600-Rh	128	64.66	30.76	4.50 (Fe)	0.08 (Rh)
Fe-Mg-Al-600-Pt	122	64.68	30.70	4.57 (Fe)	0.05 (Pt)

The loading of noble metals introduced into the Cu-Mg-Al-600 and Fe-Mg-Al-600 samples is very low in comparison to the content of copper and iron. Thus, also the intensity of the bands characteristic of noble metal species is significantly lower than the intensity of the peaks related to the presence of copper or iron species. Therefore, the UV–vis–DR spectra recorded for the Cu-Mg-Al-600 and Fe-Mg-Al-600 samples and their modifications with noble metals (not shown) are very similar and discussion on any possible small differences is very speculative.

TPR studies were performed for all the catalysts. For the Mg-Al-600 sample and its derivatives with platinum and palladium only very weak and broad peaks related probably to the hydrogenation of residual carbonates was detected (not shown). For the Mg-Al-600-Rh catalyst an intensive reduction peak related to reduction of rhodium present in the $MgRh_2O_4$ phase was detected at about 410 °C (Fig. 5). The rhodium content in the sample is very low and therefore such phase was not identified in XRD analysis. Formation of the $MgRh_2O_4$ phase during the calcination of MgO-supported Rh samples was reported earlier in the scientific literature [e.g. 20,21]. The small peak located at about 150 °C is probably attributed to the reduction of rhodium oxide (RhO_x) species deposited on the support surface. Reduction of such species was reported to proceed at temperature below 200 °C [e.g. 20]. While the weak and broad peak at about 900 °C is probably related to the hydrogenation of residual carbonates, which were also detected by TG–DTA-QMS measurements.

The results of TPR studies of the Cu-Mg-Al-600 catalyst and its modifications with noble metals are presented in Fig. 5. The reduction of copper oxide species to metallic copper is represented by a sharp peak centred at about 290 °C [e.g. 22]. Introduction of the noble metals into the Cu-Mg-Al-600 sample shifted the position of that peak to lower temperatures by about 30–35 °C. Various explanations of this effect were proposed in the literature, however all are based on metal–metal interaction [23]. One of possible explanation is related to the formation of bimetallic species containing noble metals, which are reduced at temperatures lower than pure CuO phase. [e.g. 20,24–26]. It is well known that noble metals are able to the dissociative hydrogen adsorption. Such reactive atomic hydrogen can migrate (spill-over) and reduce copper oxide species at significantly lower temperatures [25,27]. The other peaks present in the TPR curves (Fig. 5) are significantly less intensive. For the Rh-containing catalyst the peak at 450 °C, related to reduction of rhodium present in the $MgRh_2O_4$ phase, was identified [e.g. 20,21]. The negative detector signal observed for the palladium containing sample at temperatures below 100 °C could be attributed to desorption of hydrogen chemisorbed on the palladium surface or absorbed in the bulk of metallic palladium particle (i.e. β-Pd hydride) [e.g. 28,29]. The other peaks, found in the TPR profiles at about 580 and 900 °C, are related to the hydrogenation of the residual, thermally stable carbonates present in the catalyst.

The results of TPR studies obtained for the Fe-Mg-Al-600 sample and its derivatives with transition metals are shown in Fig. 6. The reduction profile of the Fe-Mg-Al-600 consists of two peaks located at about 500 and 775 °C. Additionally, an increase in the hydrogen consumption observed above 900 °C, suggests that iron present in the sample was not completely reduced in the studied temperature range. Recently, similar results were reported by Vulic et al. [30], who studied reduction of the hydrotalcite originated Fe-Mg-Al oxide systems. It was suggested that the peak located at about 500 °C is assigned to the reduction of iron in metal oxide species from Fe^{3+} to Fe^{2+}, while at higher temperatures the reduction of Fe^{2+} to Fe^0 takes place. Additionally, relatively high temperature of the iron species reduction suggests that iron is probably incorporated into the $MgFe_2O_4$ spinel phase, in which Fe^{3+} cations are more stable than in the other possible iron oxide species [30]. Taking into account a large excess of magnesium over iron in the sample (atomic ration of Mg/Fe is 66/5) this hypothesis seems to be acceptable also in the case of our studies. The small content of iron in the sample and possibly low crystallinity of the spinel phase could be responsible for the lack of the corresponding reflections in diffractogram of the Fe-Mg-Al-600 catalyst. Thus, reduction peaks are probably related to the following reactions:

$$MgFe_2^{III}O_4 + H_2 = Mg_{1-x}Fe_x^{II}O + H_2O \quad (4a)$$

$$Mg_{1-x}Fe_x^{II}O + H_2 = Fe^0 + MgO + H_2O \quad (4b)$$

Modification of the Fe-Mg-Al-600 sample with noble metals resulted in an appearance of the low-temperature reduction peaks. This effect was reported in the scientific literature and was explained mainly by dissociation of H_2 molecules on the noble metal surface. Reactive atomic hydrogen can migrate (spill-over) and reduce iron oxide species at relatively low temperatures [e.g. 31]. Moreover, a peak at 420 °C, observed for the Fe-Mg-Al-600-Rh sample, is probably related to the reduction of rhodium present in the $MgRh_2O_4$ phase [e.g. 20,21]. The evolution of hydrogen (negative detector signal) observed for the palladium containing sample at temperatures below 120 °C, as it was already mentioned, is probably related to desorption of hydrogen chemisorbed on the palladium surface or absorbed in the bulk of metallic palladium particle (i.e. β-Pd hydride) [e.g. 28,29].

The obtained samples were tested in the role of the catalysts of selective oxidation of ammonia. Fig. 7 presents the results of activity experiment performed in the absence of catalyst. The ammonia conversion started at temperature as high as 375 °C and at 500 °C did not exceed 20%. The results of the catalytic tests performed for the Mg-Al-600 sample and its derivatives with noble metals are shown in Fig. 8. The ammonia conversion started at

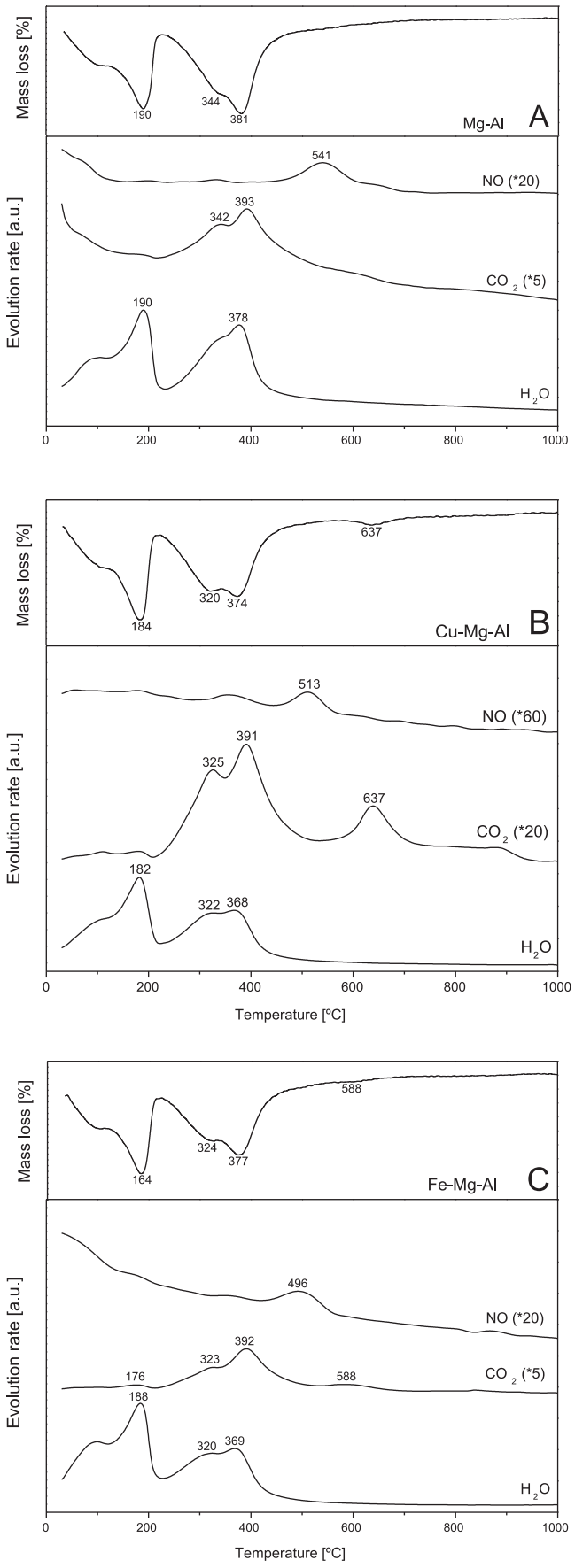

Fig. 3. DTG and QMS patterns of H_2O, CO_2, NO evolution during the thermal decomposition of Mg-Al (A), Cu-Mg-Al (B), Fe-Mg-Al (C) hydrotalcites: T = RT – 1000 °C; β = 10 °C/min; flow of pure argon (80 cm^3/min); samples = 20 mg.

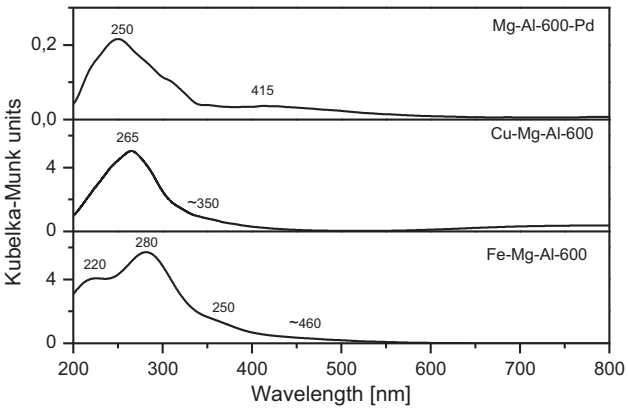

Fig. 4. UV–vis–DR spectra of the Mg-Al-600-Pd Cu-Mg-Al-600 and Fe-Mg-Al-600 samples.

temperature above 200 °C and slowly increased up to 500 °C. Nitrogen was the main product of ammonia oxidation, however also significant contribution of NO and N_2O in the reaction products was found. Deposition of noble metals on the Mg-Al-600 sample resulted in its activation in the process of ammonia oxidation but also an increase in the selectivity towards nitrogen oxides (NO and N_2O). The Mg-Al-600 catalyst presented rather poor activity, however it should be noted that the ammonia conversion was significantly higher than for the process performed without catalyst. Thus, despite the Mg-Al-600 sample does not contain any transition metals, it presents the moderate catalytic activity in the ammonia oxidation process. Platinum doped sample was found to be the most active catalyst in the series based on Mg-Al-600 support. Ammonia oxidation started at about 100 °C and temperature of 325 °C was sufficient for its complete conversion in the reaction mixture. Selectivity to nitrogen was in the range of 40–70% at temperature below 450 °C but at higher temperature drastically dropped due to the formation of significant amount of NO, which become the main reaction product. Such complex profiles of the selectivity curves observed for the Mg-Al-600-Pt catalyst is related to the complexity of the SCO process, which consists of few consecutive and parallel steps. The rate of the ammonia oxidation in the low temperature range is low and therefore, there is a significant excess of ammonia, which in a subsequent step can reduce NO to N_2 and possibly also N_2O. At higher temperatures the rate of the ammonia oxidation to NO increases and amount of residual ammonia is too small for the complete reduction of nitrogen oxide, therefore the selectivity to N_2 decreases and selectivity to NO increases. An increase in the NO selectivity observed at temperature above 350 °C could be related to the conversion of ammonia on the surface of Mg-Al oxide (cf. results for Mg-Al-600) as well as in gas phase (cf. Fig. 7). Finally, the drop in the N_2 selectivity above 425 °C could be related to the nearly complete oxidation of ammonia into NO, and therefore very limited the subsequent process of NO reduction by ammonia. Of course, the shapes of the selectivity profiles are different for various catalysts and depend on their properties, which influence the rate of the individual reaction steps.

The catalysts doped with palladium and rhodium were slightly less active and temperature of 350–370 °C was needed for the complete oxidation of ammonia in the reaction mixture. Nitrogen was the main reaction product at temperatures below 500 °C, however selectivity to N_2 was relatively low and did not exceed 60 and 75% for Mg-Al-600-Pd and Mg-Al-600-Rh, respectively. The modifications of the catalytic performance of the Mg-Al-600 sample by noble metals are consistent with our expectations because noble metals are know to be active catalysts of ammonia oxidation to NO [e.g. 32]. As it was shown by TPR studies, part of rhodium introduced into

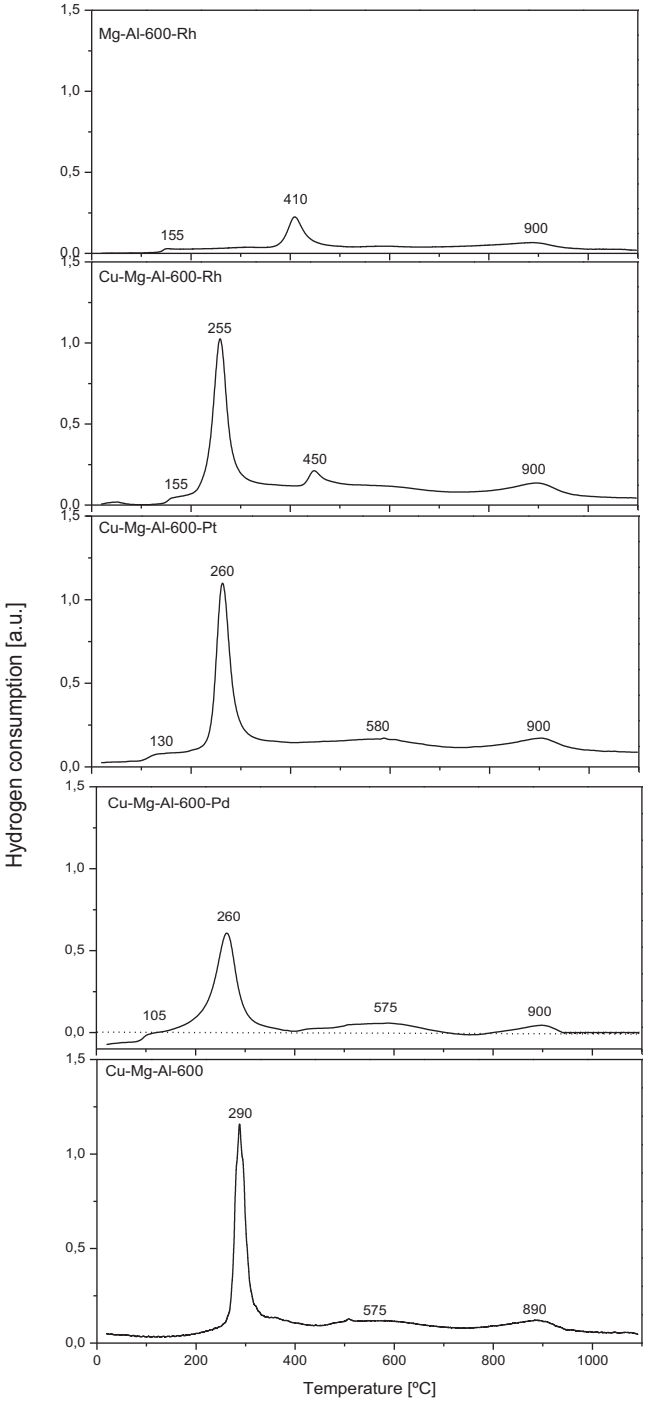

Fig. 5. Results of H_2-TPR studies for the Mg-Al-600-Rh sample and a series of the Cu-Mg-Al-600 catalysts modified with noble metals.

calcined hydrotalcites formed the Rh_2MgO_4 spinel phase, which needs higher temperatures to act as the redox centre then other noble metal species [20,21]. It could explain the higher selectivity to nitrogen obtained in the presence of Mg-Al-600-Rh than those determined for the samples containing platinum and palladium.

Recently, the studies of ammonia oxidation over Pt, Pd and Rh wires by temporal analysis of products (TAP) and density functional theory (DFT) calculations were reported by Pérez-Ramírez et al. [33]. It was shown that all these noble metals are catalytically active not only in direct oxidation of NH_3 into NO but also in the secondary transformation of nitric oxide to N_2 and N_2O. However, the catalytic activity of the studied noble metals in the secondary

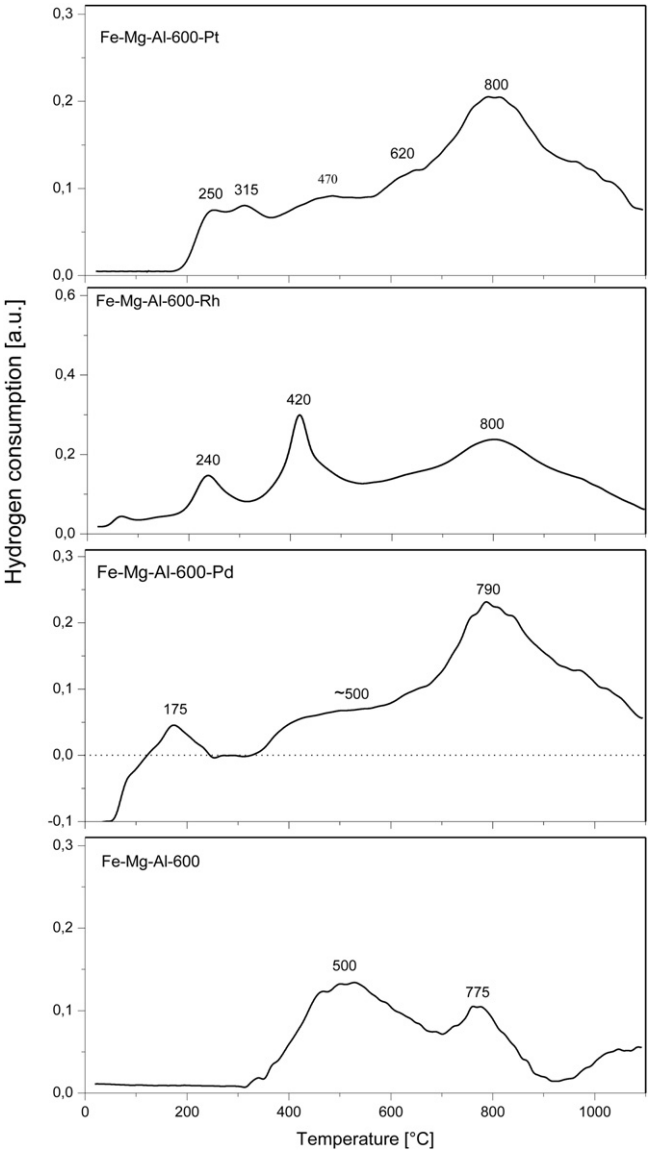

Fig. 6. Results of H_2-TPR studies for the Fe-Mg-Al-600 sample and its modifications with noble metals.

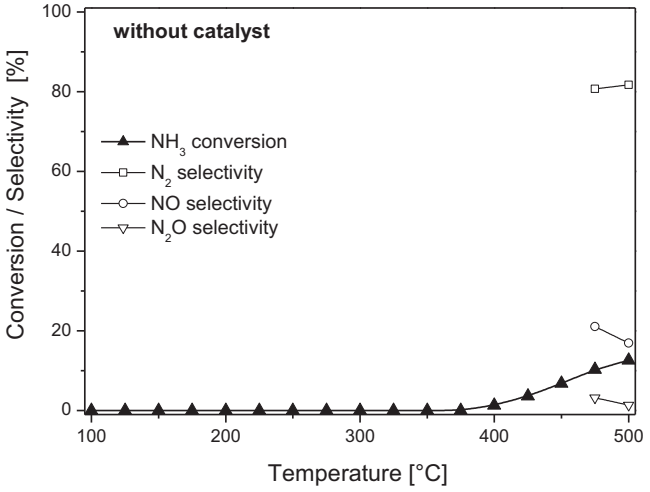

Fig. 7. Results of activity tests for the SCO process performed in the absence of catalyst performed. [NH_3] = 0.5%, [O_2] = 2.5%, [He] = 97%, total flow rate = 40 cm^3/min.

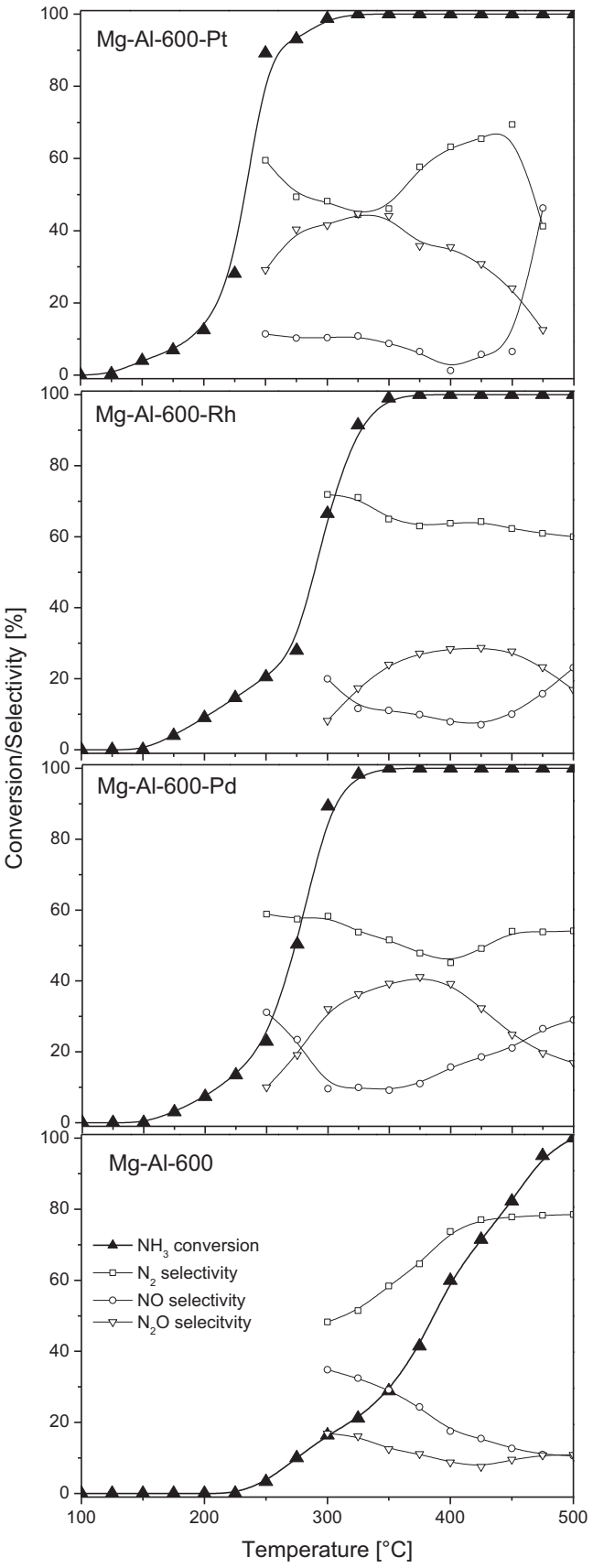

Fig. 8. Results of catalytic tests performed for Mg-Al calcined hydrotalcite and its modifications with noble metals. Conditions: catalysts = 100 mg, [NH_3] = 0.5%, [O_2] = 2.5%, [He] = 97%, total flow rate = 40 cm^3/min.

process of N_2 and N_2O formation is significantly different. It was found that rhodium is the most active catalyst for the reduction of nitric oxide by ammonia, followed by palladium, while platinum is the least active one. These experimental results were in line with DFT calculations performed for the selected planes of these noble metals. Additionally, DFT calculations have shown that the N_2O formation over Rh (1 0 0) plane needs higher activation energy than over Pt (1 0 0) or Pd (1 0 0). Of course, the DFT calculations were performed for the selected, model planes of noble metals, while TAP experiments were done for noble metals wires at temperature as high as 800 °C but results of these studies are fully consistent with the results of our activity tests performed for the catalysts containing only very small amounts of Pt, Pd or Rh deposited on the surface of mixed Mg-Al oxide at temperatures below 500 °C. Another interesting effect was observed for the Mg-Al-600-Pt and Mg-Al-600-Pd catalysts. For both samples an increase in the reaction temperature to 350–400 °C resulted in gradual decrease of selectivity to N_2, while at higher temperatures contribution of nitrogen in the reaction products increased (for Mg-Al-600-Pt only to 450 °C). This effect could be explained by an increasing role of the secondary reaction of NO reduction by ammonia over Mg-Al oxide support (cf. Fig. 8, Mg-Al-600) or in the gas phase (cf. Fig. 7) at elevated temperatures. This effect was not observed for the Mg-Al-600-Rh catalyst, which was found to be significantly more selective to nitrogen comparing to the samples doped with palladium or platinum.

Fig. 9 presents the results of the catalytic tests performed for the Cu-Mg-Al-600 sample and its derivatives containing noble metals. It should be noted that the Cu-Mg-Al-600 catalyst is significantly more active than the Mg-Al-600 sample, what proves a very important role of copper oxide species in this process. Oxidation of ammonia was observed from about 200 °C, while temperature of 425 °C was needed for the complete conversion of NH_3 in the reaction mixture. It should be noted that selectivity to N_2 was very high and did not drop below 90% at the studied temperature range. As it was shown by UV–vis–DRS studies copper was present mainly in the form of monomeric and small clustered species dispersed in the Mg-Al oxide matrix in the Cu-Mg-Al-600 sample. The presence of such copper species, which are known to be active in the DeNOx process and on the other hand their catalytic activity in the ammonia oxidation process is lower in comparison to bulky copper oxide species [e.g. 7,10], are responsible for high selectivity to nitrogen.

An increase in the catalytic activity of the Cu-Mg-Al-600 sample was observed after its modification with small amounts of noble metals. The highest activity was found for the sample doped with platinum (Cu-Mg-Al-600-Pt), which was able to completely oxidize ammonia at temperature as low as 350 °C. The Pd- and Rh-containing catalysts were less active and temperature higher by about 50 °C was necessary for the complete elimination of ammonia from the reaction mixture. Unfortunately, an increase in the catalytic activity was accompanied by a decrease in the selectivity to nitrogen. However, it should be noted that the selectivity to nitrogen is significantly higher for a series of the catalyst based on Cu-Mg-Al-600 than for noble metals deposited on Mg-Al-600. This effect could be explained by the presence of copper oxide species, which are known to be active components of the catalysts for selective reduction of NO by ammonia to nitrogen and water vapour [e.g. 7,10]. Thus, NO produced by ammonia oxidation (Eq. (2)) is in the subsequent step reduced by residual NH_3 (Eqs. (3a) and (3b)). In a group of the Cu-Mg-Al-600 samples modified with noble metals, the highest selectivity to nitrogen, which was above 85% in the studied temperature range, was obtained for the Rh-containing catalyst. As it was mentioned above, it could be related to the presence of the Rh_2MgO_4 spinel phase, which needs higher temperatures to act as the redox centre than other noble metal species [20,21] and therefore the oxidation of ammonia to NO is less effective and the

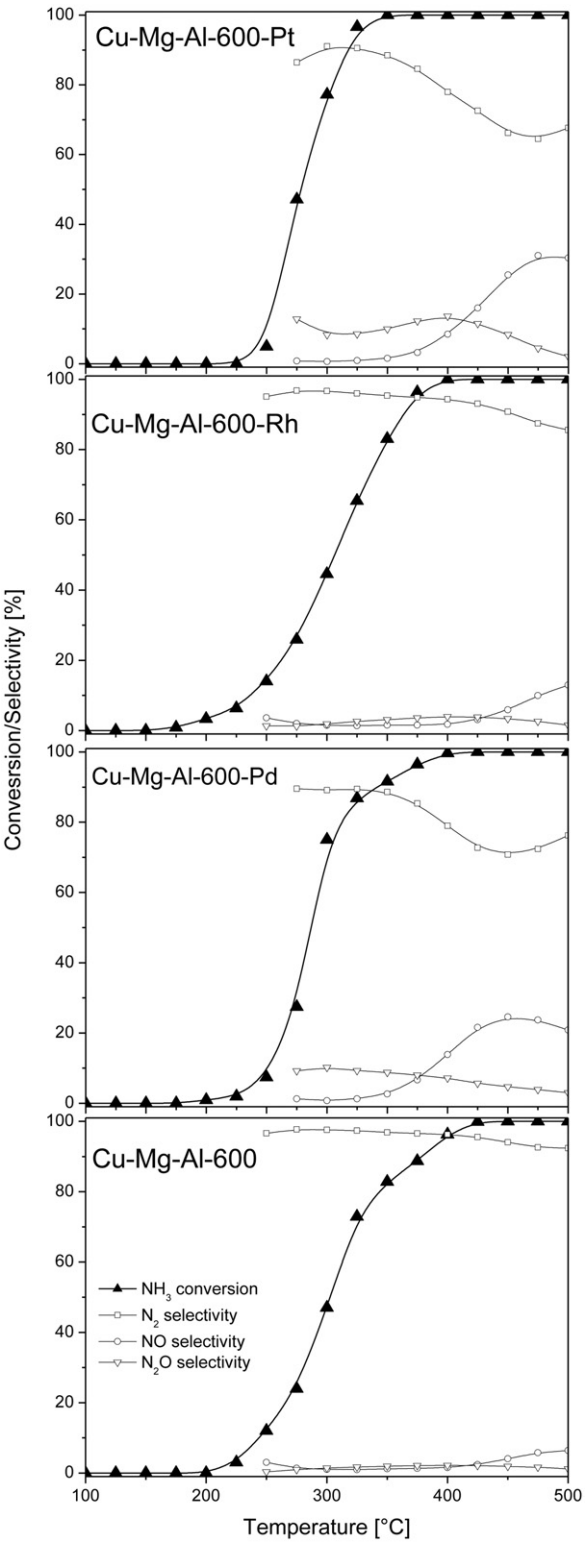

Fig. 9. Results of catalytic tests for the SCO process performed over Cu-Mg-Al calcined hydrotalcite and its modifications with noble metals. Conditions: catalysts = 100 mg, [NH_3] = 0.5%, [O_2] = 2.5%, [He] = 97%, total flow rate = 40 cm^3/min.

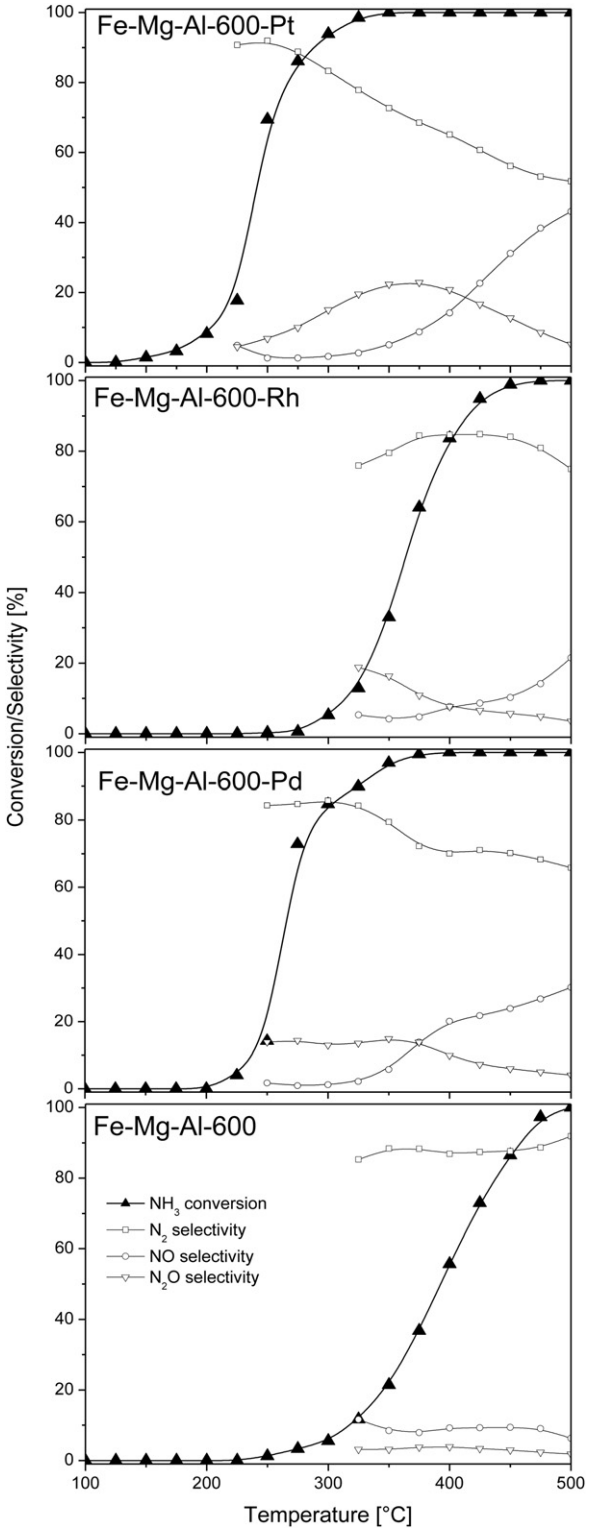

Fig. 10. Results of catalytic tests for the SCO process performed over Fe-Mg-Al calcined hydrotalcite and its modifications with noble metals. Conditions: catalysts = 100 mg, [NH_3] = 0.5%, [O_2] = 2.5%, [He] = 97%, total flow rate = 40 cm^3/min.

selectivity to nitrogen higher than for the other catalysts of this series.

The results of the catalytic tests performed in the presence of the Fe-Mg-Al-600 catalyst and its derivatives containing noble metals are shown in Fig. 10. The catalytic activity of the Fe-Mg-Al-600 sample in the process of ammonia oxidation is only slightly better than that determined for Mg-Al-600. However, it should be noted that the Fe-containing catalyst presented much higher selectivity to nitrogen. As it was shown by TPR studies, iron is present mainly in the form of the $MgFe_2O_4$ spinel phases in a series of the Fe-Mg-Al-600 samples. Fe^{3+} ions in such spinel phase are reduced at higher temperature than in the other iron oxide species [30] and

therefore, higher temperature is needed for their activation in the redox processes.

Deposition of noble metals significantly increased its catalytic activity and decreased selectivity to N_2. In this series of the samples the best catalytic activity was found for the Fe-Mg-Al-600-Pt catalyst, which was able to oxidize ammonia completely in the reaction mixture at temperature of 350 °C. Less active were the Pd- and Rh-containing catalysts, which needed temperatures at least 400 and 475 °C, respectively, for the total conversion of ammonia. Deposition of noble metals on Fe-Mg-Al-600 decreased its selectivity to nitrogen. This effect was more significant than for the series of the catalysts based on the Cu-Mg-Al-600 sample but less significant than for the series based on the Mg-Al-600 support. Iron oxide phases are known to be catalytically active in the selective reduction of NO with ammonia [e.g. 7,10]. However, iron oxide species operate at higher temperatures than the Cu-containing catalysts [e.g. 7,10]. Thus, it seems that at temperatures of the iron catalyst operation, the rate of ammonia oxidation to NO is very high and the amount of residual ammonia is too small for the complete reduction of nitrogen oxide to N_2 and H_2O.

The results of the catalytic tests were summarized in Table 3, which presents temperatures needed for 50 and 100% of ammonia conversion as well as the selectivity to nitrogen at these temperatures.

It was suggested that the SCO process over the studied catalysts proceeds according to the internal SCR (*i-SCR*) mechanism. Therefore, these catalysts should be also active in the process of the selective catalytic reduction of NO with ammonia (DeNOx). Results of the catalytic studies of the DeNOx process for a series of the copper containing samples are presented in Fig. 11. N_2 and N_2O were the only detected nitrogen containing reaction products. It can be seen that all test samples are active catalysts of the DeNOx process. The NO conversion started at about 150 °C and increased to 75% at 325 °C in the presence of the Cu-Mg-Al-600 catalyst. At higher temperatures, the NO conversion decreased due to the side process of ammonia oxidation. In general, deposition of noble metals enhanced activity of the catalysts in the side process of ammonia oxidation and decreased selectivity to nitrogen. Additionally, the DeNOx process proceeded at lower temperatures in the presence of the Cu-Mg-Al-600-Pt and Cu-Mg-Al-600-Pd catalysts than Cu-Mg-Al-600, but also these catalysts were very active in the side reaction of direct ammonia oxidation.

As it was mentioned above, noble metal species are responsible for the oxidation of ammonia to NO in the SCO process. Their activity in this reaction is related to chemisorption, dissociation and activation of oxygen for the reaction with ammonia molecules. There are some reports proposing the subsequent dehydrogenation ($-NH_3 \rightarrow -NH_2 \rightarrow -NH \rightarrow -N$) and finally oxidation of chemisorbed ammonia into NO [e.g. 34–37] or even NO_2 [1] or recombination of surface nitrogen atoms to N_2 [6] over noble

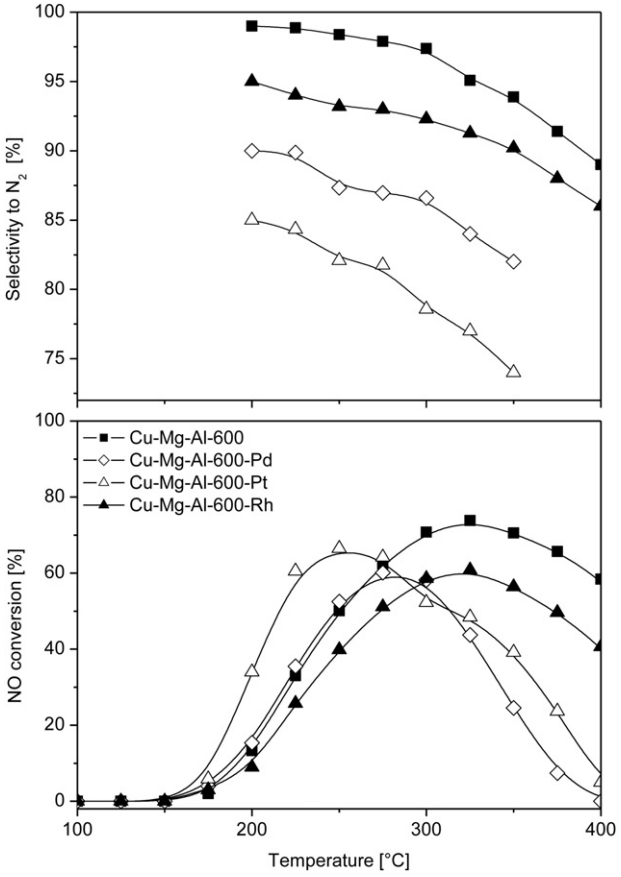

Fig. 11. Results of catalytic tests for the DeNOx process performed for Cu-Mg-Al calcined hydrotalcite and its modifications with noble metals. Conditions: catalysts = 100 mg, [NH_3] = 0.5%, [O_2] = 2.5%, [He] = 97%, total flow rate = 40 cm^3/min.

metals. On the other hand, copper oxide species are less active in ammonia oxidation than noble metals. Thus, dehydrogenation of chemisorbed NH_3 molecules is probably much slower, and therefore the significant population of $-NH_{3-x}$ species on their surface could be expected [1]. Such species can react with NO to form N_2 or/and N_2O molecules. [e.g. 35,36,38,39]. Recently, Cui et al. [6], who studied the catalytic system containing RuO_2 and CuO proposed synergistic catalytic effect between these components during the ammonia oxidation reaction. Authors suggested that coordinatively unsaturated Ru atoms (cus), present in RuO_2 can easy adsorb and activated NH_3 molecules and oxygen atoms. Such adsorbed species can be converted in a sequence of the following reactions:

$$NH_{3-cus} + O_{-cus} \rightarrow (NH_2)_{ad} + OH_{ad} \rightarrow N_{-cus} + H_2O \quad (5a)$$

Table 3
Comparison of the results of catalytic tests ($T_{50\%}$ and $T_{100\%}$ temperatures needed for 50% and 100% of NH_3 conversion, respectively).

Catalyst	$T_{50\%}$ [°C]	N_2 selectivity at $T_{50\%}$ [%]	$T_{100\%}$ [°C]	N_2 selectivity at $T_{100\%}$ [%]
Without catalyst				
Mg-Al-600	387	68	506	78
Mg-Al-600-Pd	374	57	362	50
Mg-Al-600-Rh	289	72	387	64
Mg-Al-600-Pt	233	61	338	46
Cu-Mg-Al-600	303	97	437	94
Cu-Mg-Al-600-Pd	287	89	413	76
Cu-Mg-Al-600-Rh	305	96	415	93
Cu-Mg-Al-600-Pt	279	87	366	86
Fe-Mg-Al-600	392	98	510	92
Fe-Mg-Al-600-Pd	268	85	407	70
Fe-Mg-Al-600-Rh	364	82	486	79
Fe-Mg-Al-600-Pt	241	91	362	71

In the next step the N_{-cus} species may recombine with each other to form N_2 (5b) or with O_{-cus} into NO_{-cus} (5c):

$$N_{-cus} + N_{-cus} \rightarrow N_2 \quad (5b)$$

$$N_{-cus} + O_{-cus} \rightarrow NO_{-cus} \quad (5c)$$

Thus, the activity and selectivity of the process depends on density and distribution of the N_{-cus} and O_{-cus} species on the catalyst surface. Cui et al. [6] suggested also that, CuO can selectively reduce NO_{-cus} species adsorbed on the RuO_2 surface to N_2:

$$NO_{-cus} + NH_{3-cus} \rightarrow N_2 + H_2O \quad (4d)$$

This mechanism was proposed for mesoporous Cu-Ru bimetallic oxide system, however it seems that it could be valid also in case of the other combinations of noble metals with CuO.

Of course, there is still discussion related to the possible mechanisms of the ammonia oxidation process over various types of catalysts and more detailed studies are necessary for the explanation of this issue.

4. Summary

Cu-containing mixed oxides were found to be active and selective catalysts of the low-temperature ammonia oxidation to nitrogen. On the other hand calcined Fe-Mg-Al hydrotalcite was catalytically active only in the high temperature range. Modification of these catalysts with noble metals (Pt, Pd, Rh) activated them for the low-temperature SCO reaction but also decreased their selectivity to nitrogen. This negative effect of noble metal deposition was more significant for a series of the Fe-containing catalysts. The catalytic performance of the studied catalysts was assigned to the activity of noble metals in ammonia oxidation to NO and activity of the copper and iron oxide species in the process of NO reduction with ammonia to N_2 and N_2O. The relative reaction rate both these processes determines the activity and selectivity of the catalytic systems in the SCO reaction.

Acknowledgement

Part of the research was done with equipment purchased in the frame of European Regional Development Fund (Polish Innovation Economy Operational Program – contract no. POIG.02.01.00-12-023/08).

References

[1] G. Olofsson, A. Hinz, A. Anderson, Chemical Engineering Science 59 (2004) 4113–4123.
[2] Y. Li, J.N. Armor, Applied Catalysis B 13 (1997) 131–139.
[3] M. Amblard, R. Burch, B.W.L. Southward, Applied Catalysis B 22 (1999) L159–L166.
[4] P.D. Sobczyk, E.J.M. Hensen, A.M. de Jong, A.S. van Santen, Topics in Catalysis 23 (2003) 109–117.
[5] R.Q. Long, R.T. Yang, Catalysis Letters 78 (2002) 353–357.
[6] X. Cui, J. Zou, Z. Ye, H. Chen, L. Li, M. Ruan, J. Shi, Journal of Catalysis 270 (2010) 310–317.
[7] L. Chmielarz, P. Kuśtrowski, A. Rafalska-Łasocha, D. Majda, R. Dziembaj, Applied Catalysis B 35 (2002) 195–210.
[8] B. Montanari, A. Vaccari, M. Gazzano, P. Käßner, H. Papp, J. Pasel, R. Dziembaj, W. Makowski, T. Łojewski, Applied Catalysis B 13 (1997) 205–217.
[9] L. Chmielarz, M. Rutkowska, P. Kuśtrowski, M. Drozdek, Z. Piwowarska, B. Dudek, R. Dziembaj, M. Michalik, Journal of Thermal Analysis and Calorimetry 105 (2011) 161–170.
[10] L. Chmielarz, Z. Piwowarska, M. Rutkowska, M. Wojciechowska, B. Dudek, S. Witkowski, M. Michalik, Catalysis Communication 17 (2012) 118–125.
[11] L. Chmielarz, A. Węgrzyn, M. Wojciechowska, S. Witkowski, M. Michalik, Catalysis Letters 141 (2011) 1345–1354.
[12] L. Chmielarz, P. Kuśtrowski, A. Rafalska-Łasocha, R. Dziembaj, Applied Catalysis B 58 (2005) 235–244.
[13] A. Węgrzyn, A. Rafalska-Łasocha, D. Majda, R. Dziembaj, H. Papp, Journal of Thermal Analysis and Calorimetry 99 (2010) 443–457.
[14] A.S. Ivanova, E.M. Slavinskaya, R.V. Gulyaev, V.I. Zaikovskii, O.A. Stonkus, I.G. Danilova, L.M. Plyasova, I.A. Polukhina, A.I. Boronin, Applied Catalysis B 97 (2010) 57–71.
[15] F.M.T. Mendes, M. Schmal, Applied Catalysis A 151 (1997) 393–408.
[16] M.C. Marion, E. Grabowski, M. Primet, Journal of the Chemical Society-Faraday Transactions 86 (1990) 3027–3032.
[17] J. Shen, B. Guang, M. Tu, Y. Chen, Catalysis Today 30 (1996) 77–82.
[18] M.A. Wojtowicz, J.R. Pels, J.A. Moulijn, Fuel Processing Technology 34 (1993) 1–71.
[19] Y. Ohishi, T. Kawabata, T. Shishido, K. Takaki, Q. Zhang, Y. Wang, K. Nomura, K. Takehira, Applied Catalysis A 288 (2005) 220–231.
[20] E. Ruckenstein, H.Y. Wang, Applied Catalysis A 198 (2000) 33–41.
[21] N. Palmeri, S. Cavallaro, V. Chiodo, S. Freni, F. Frusteri, J.C.J. Bart, International Journal of Hydrogen Energy 32 (2007) 3335–3342.
[22] P. Reyes, M. Oportus, G. Pecchi, Catalysis Letters 37 (1996) 193–197.
[23] W.P. Dow, Y.P. Wang, T.J. Huang, Journal of Catalysis 160 (1996) 155–170.
[24] J.M. Thomas, R. Raja, B.F.G. Johnson, S. Hermans, M.D. Jones, T. Khimyak, Industrial and Engineering Chemistry Research 42 (2003) 1563–1570.
[25] A. Benedetti, G. Fagherazzi, F. Pinna, G. Rampazzo, M. Selva, G. Strukul, Catalysis Letters 10 (1991) 215–223.
[26] J. Batista, A. Pintar, D. Mandrino, M. Jenko, V. Martin, Applied Catalysis A 206 (2001) 113–124.
[27] F. Gauthard, F. Epron, J. Barbier, Journal of Catalysis 220 (2003) 182–191.
[28] P. Claus, H. Berndt, C. Mohr, J. Radnik, E.J. Shin, M.A. Keane, Journal of Catalysis 192 (2000) 88–97.
[29] G. Strukul, F. Pinna, M. Marella, L. Meregalli, M. Tomaselli, Catalysis Today 27 (1996) 209–214.
[30] T.J. Vulic, A.F.K. Reitzmann, K. Lázár, Chemical Engineering Journal doi:10.1016/j.cej.2012.06.152.
[31] F.J. Berry, L.E. Smart, P.S.S. Prasad, N. Lingaiah, P.K. Rao, Applied Catalysis A 204 (2000) 191–201.
[32] T. Pignet, L.D. Schmidt, Journal of Catalysis 40 (1975) 212–225.
[33] J. Pérez-Ramírez, E.V. Kondratenko, G. Novell-Leruth, J.M. Ricart, Journal of Catalysis 261 (2009) 217–223.
[34] J. Pérez-Ramírez, E.V. Kondratenko, V.A. Kondratenko, M. Baerns, Journal of Catalysis 229 (2005) 303–313.
[35] T. Katona, L. Guczi, G.A. Somorjai, Journal of Catalysis 135 (1992) 434–443.
[36] T. Katona, G.A. Somorjai, Journal of Physical Chemistry 96 (1992) 5465–5472.
[37] A.P. Seitsonen, D. Crihan, M. Knapp, A. Resta, E. Lundgren, J.N. Andersen, H. Over, Surface Science 603 (2009) L113–L116.
[38] K. Otto, M. Shelef, J.T. Kummer, Journal of Physical Chemistry 74 (1970) 2690–2696.
[39] K. Otto, M. Shelef, J.T. Kummer, Journal of Physical Chemistry 75 (1971) 875–879.